CHARACTERIZATION AND FABRICATION OF HIGH-DENSITY, ON-DEMAND, REUSABLE, IN-PLANE POLYMER INTERCONNECTS TOWARDS STANDARDIZED MICROFLUIDIC PACKAGING

Ronalee Lo[1] and Ellis Meng[1]

[1]Department of Biomedical Engineering, University of Southern California, USA

ABSTRACT

The first on-demand, high-density, reusable, in-plane interconnects that can be integrated with microfluidic systems are presented. Interconnects are arrayed for high-density microfluidic packaging. The self-sealing nature and mechanical robustness of in-plane connections allow fluidic connections to be repeatedly broken and re-established [1]. Mechanical characterized through insertion/removal force measurements, finite-element-modeling (FEM) and real-time photoelastic stress distribution studies is presented.

KEYWORDS: Packaging, interconnect, world-to-chip, microfluidics

INTRODUCTION

The full potential of micro total analysis systems (μTAS) and lab-on-a-chip (LOC) microfluidic devices is limited by the lack of standardized and reliable packaging between the micro and macro worlds. Current micro-to-macro world connection methods are custom-made solutions which require adhesives, complicated fabrication steps, precise alignment, and extensive manual labor.

We present reusable and arrayed microfluidic interconnects created using standard batch microfabrication techniques and integrated in-plane with microfluidic devices (Fig. 1). A "pin-and-socket" approach was used where commercially-available non-coring needles (33G) puncture polydimethylsiloxane (PDMS) septa to establish access to the microfluidic system. First, a surface micromachined channel was created in either SU-8 [1] or Parylene (Fig. 2A-C). SU-8 was spun and patterned to create mechanical anchors and filled with PDMS to create the septa (Fig. 2D, E). The system was capped with a glass plate to enclose the microfluidic system (Fig. 2F).

Interconnects consist of an anchor and septum at each inlet/outlet (Fig. 3A). Needle arrays held fixed in a polymer housing are manually inserted through the septa (Fig. 3B). The in-plane design utilizes a standard center-to-center spacing between needles (2.54mm and 1mm).

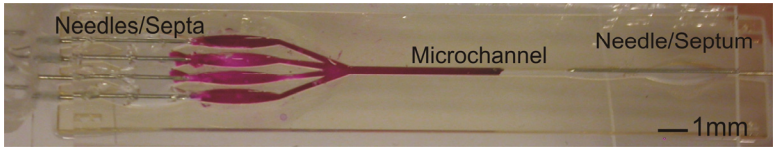

Figure 1. Microfluidic device with integrated interconnect. Fluid is introduced into the microchannel via a needle array which pierces the setpa.

978-0-9798064-1-4/μTAS2008/$20©2008CBMS

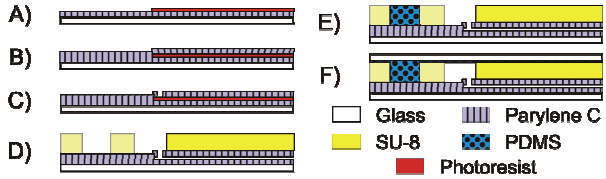

Figure 2. Fabrication steps for integrated interconnect.

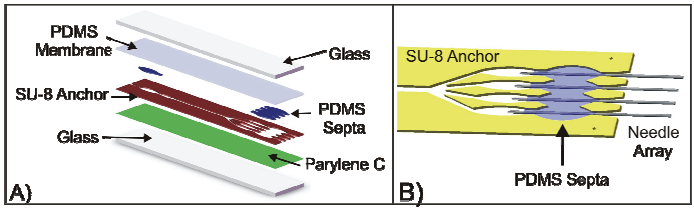

Figure 3. Exploded Solidworks illustration of a) a multiple interconnect assembly. b) Close-up image of an assembled multiple interconnect setup.

THEORY AND EXPERIMENTAL

Insertion force, $f_{insertion}$, is the force necessary to puncture the PDMS septum with a needle array; it is composed of three main components [2]:

$$f_{insertion} = f_{stiffness} + f_{cutting} + f_{friction} \quad (1)$$

The stiffness force ($f_{stiffness}$) is due to material deformation pre-puncture. Post-puncture, the needle experiences a combination of cutting force ($f_{cutting}$), the force required to push through the material, and frictional force ($f_{friction}$). The force necessary to puncture the septum (PDMS slab measuring 2 ± 0.1mm thick) with a single 33G needle and needle arrays (4 or 8 33G needles, 2.54mm spacing), was measured.

The stress distribution within the septum during insertion was modeled using FEM analysis of constrained PDMS. The FEM results were validated with photoelastic imaging. Stress in PDMS results in a visible phase difference (Δ) and is proportional to principle stresses (σ_x, σ_y), wavelength (λ), stress-optical coefficient (C), and material thickness (h) [3]:

$$\Delta = \frac{2\pi h}{\lambda} C(\sigma_x - \sigma_y) \quad (2)$$

RESULTS AND DISCUSSION

The various forces components for single needle and needle array implementation (4 and 8 needles) were measured (Table 1). Stiffness force of the needle arrays could not be measured due to equipment resolution and lack of simultaneous tip contact with the PDMS surface. In general, forces scaled with the needle number, effectively limiting the maximum interconnect density due to mechanical robustness and the range of practical forces needed to manually insert a dense needle array.

FEM of the stress distribution during needle insertion of single and arrayed interconnects was performed using measured forces (Fig. 4). Photoelastic imaging confirmed FEM results. The maximum stress in the FEM analysis is approximately 22% of the tensile strength of PDMS, indicating no critical failure locations. Fur-

thermore, the compliant PDMS septa localizes stresses around the needle and thus minimizes stress transmission to the anchors.

Table 1. Measured forces (mean ± SE, n=4) for needle insertion into and removal from a PDMS slab.

Force [N]	Single Needle (33G)	Needle Array (Four 33G Needles)	Needle Array (Eight 33G Needles)
Stiffness	-0.18 ± 0.016	N/A	N/A
Max Insertion	-0.87 ± 0.022	-3.30 ± 0.050	-5.58 ± 0.171
Cutting	-0.22 ± 0.053	-0.36 ± 0.099	-0.85 ± 0.023
Frictional	-0.65 ± 0.069	-2.94 ± 0.056	-4.73 ± 0.190
Removal	0.60 ± 0.029	2.65 ± 0.066	4.54 ± 0.150

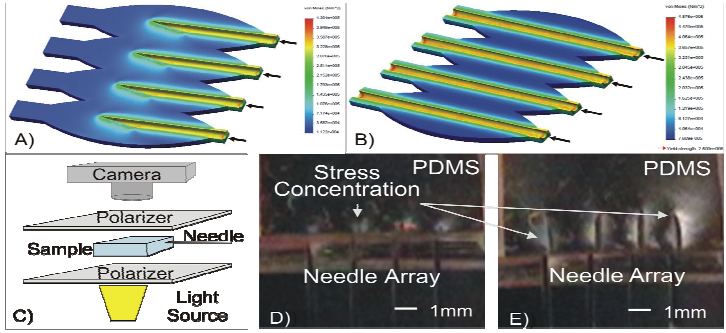

Figure 4. Stress distribution in PDMS septa during needle array insertion using FEM analysis: a) partially inserted and b) through. c) Polarized stress imaging set-up and d, e) photoelastic imaging of stresses in PDMS.

CONCLUSIONS

The fabrication and characterization of a novel on-demand method for integrating robust and high-density interconnects to microfluidic systems is presented. Both mechanical modeling and experimental validation were performed. These interconnects offer a practical solution for standardizing microfluidic connections.

ACKNOWLEDGEMENTS

This work was funded in part by an NSF CAREER grant (EEC-0547544). The authors would like to thank Dr. Donghai Zhu, Dr. James C. Eckert, Dr. David A. Mann, Mr. Merrill Roragen, and members of the Biomedical Microsystem Lab at the University of Southern California.

REFERENCES

[1] R. Lo and E. Meng, "Integrated and reusable in-plane microfluidic interconnects," *Sensors and Actuators B: Chemical*, vol. 132, pp. 531-539, (2008).

[2] C. Simone and A. M. Okamura, "Modeling of needle insertion forces for robot-assisted percutaneous therapy," (2002).

[3] S. Timoshenko and J. N. Goodier, *Theory of Elasticity*, 3rd ed. New York: McGraw-Hill, (1970).